Highly Condensed Epoxy−Oligosiloxane-Based Hybrid Material for Transparent Low-*k* Dielectric Coatings

SeungCheol Yang, Seung-Yeon Kwak, JungHo Jin, and Byeong-Soo Bae*

Laboratory of Optical Materials and Coating, Department of Materials Science and Engineering, Korea Advanced Institute of Science and Technology, Daejeon 305-701, Republic of Korea

ABSTRACT A highly condensed epoxy−oligosiloxane resin was synthesized using a sol−gel condensation reaction of (3-glycidoxypropyl)trimethoxysilane and diphenylsilanediol in the presence of solvent. A higher degree of condensation and a larger molecular size of oligosiloxanes were achieved compared to a condensation reaction without the addition of a solvent. The epoxy−hybrimer coating film was fabricated by the spin coating and thermal curing of the synthesized oligosiloxane resin. The leakage current density and the dielectric constant decreased from 25.9 to 7.6 nA cm^{-2} and from 3.16 to 3.03, respectively, by using the solvent in the preparation. The hybrimer coating film of a highly condensed oligosiloxane resin had a high transmittance of over 90% in a wavelength between 300 and 800 nm. Thus, the epoxy−hybrimer coating film can be utilized as the passivation layer in the thin-film transistor.

KEYWORDS: oligosiloxane • hybrid material • passivation • TFT • dielectric coating

INTRODUCTION

Thin-film transistors (TFTs) have been widely used in active matrix liquid-crystal displays (AMLCDs). In AMLCDs, the general structure of TFT is a back-channel-etch type with indium−tin oxide (ITO) pixel electrodes on top of the passivation layers. Silicon nitride (SiN_x) deposited by plasma-enhanced chemical vapor deposition (PECVD) in this structure is generally used as the passivation layers because the passivation layers fabricated by the SiN_x film have uniform thickness over the topology of TFT and good electrical properties. However, the high dielectric constant ($k \sim 7$) of the SiN_x film can cause capacitive coupling, degrading the TFT performance, and a low transmittance below 90% of the SiN_x film at the visible region can obstruct the fabrication of AMLCDs with high resolution and brightness. Furthermore, the PECVD process is not eligible to meet the requirement of cost and planarization for the large substrate size and surface topology of the substrate (1, 2). Thus, it is desirable to develop a soluble organic dielectric coating material with high insulation and transparency to replace the vacuum-deposited SiN_x passivation film in the TFT with a large substrate size. Recently, it has been reported that soluble siloxane-based low-*k* dielectric coating materials with good insulating properties and high transmittance (over 90%) can be used as a passivation layer in the TFT (3−6).

Inorganic−organic nanohybrid materials (hybrimers) based on sol−gel-derived oligosiloxane have been investigated for use in many optical applications owing to their excellent transparency and easy fabrication process (7−10). The hybrimers, in which oligosiloxanes are dispersed in the polymer matrix, are formed by polymerization of the organo−oligosiloxane resins that are synthesized by a sol−gel reaction of organosilanes. The dense molecular structure of the hybrimers, which can be obtained by the complete polymerization of highly condensed organo−oligosiloxane resins, can be expected to have a low leakage current density for the coating film to be used as the passivation layer. The electrical characteristics of the hybrimer films such as the dielectric constant can also be affected by the degree of siloxane formation and organic polymerization as well as the molecular composition. It was reported that transparent epoxy−hybrimer was fabricated by thermal curing of the epoxy−oligosiloxane resins synthesized by the sol−gel condensation reaction between (3-glycidoxypropyl)trimethoxysilane (GPTS) and diphenylsilanediol (DPSD) (11). However, the synthesized epoxy−oligosiloxane resins had a degree of condensation (DOC) as low as 70%, hardly high enough to achieve good dielectric characteristics of the hybrimer films. Thus, the production of highly condensed epoxy−oligosiloxane resins to induce the improved dielectric properties in the hybrimers is required.

In this study, we synthesized higher condensed epoxy−oligosiloxane resins in the presence of a solvent by a sol−gel condensation reaction of organosilanes. The molecular sizes and species of the synthesized epoxy−oligosiloxanes were characterized and compared to those of the epoxy−oligosiloxanes without the addition of a solvent. It was found that the electrical properties of the coating film are sensitive to the degree of siloxane formation in the epoxy−oligosiloxane resins. The coating film of higher condensed epoxy−oligosiloxane resins showed the improved dielectric characteristics to be used as the transparent passivation layer in the TFT.

* Tel: +42 82 350 4119. Fax: +82 42 350 3310. E-mail: bsbae@kaist.ac.kr.
Received for review April 10, 2009 and accepted June 15, 2009

DOI: 10.1021/am900252v

Scheme 1. Synthesis of Highly Condensed Epoxy−Oligosiloxane

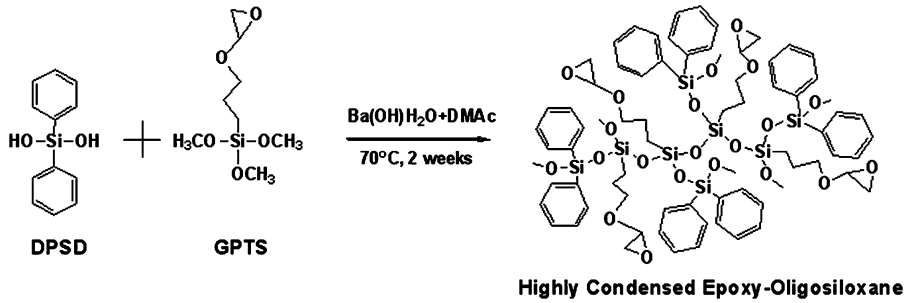

Table 1. Formulation of Epoxy−Oligosiloxane Resins

sample	GPTS	DPSD	$Ba(OH)_2 \cdot H_2O$	DMAc
GD50	11.82 g (0.05 mol)	10.81 g (0.05 mol)	0.04 g	
HGD50	11.82 g (0.05 mol)	10.81 g (0.05 mol)	0.04 g	7.8 g

EXPERIMENTAL SECTION

Synthesis of Highly Condensed Epoxy−Oligosiloxane Resins. Two epoxy−oligosiloxane resins with different molecular sizes were synthesized by a sol−gel condensation reaction of (3-glycidoxypropyl)trimethoxysilane (GPTS; 98%, Aldrich) and diphenylsilanediol (DPSD; Gelest) as precursors and barium hydroxide monohydrate [$Ba(OH)_2 \cdot H_2O$; 98%, Aldrich] as the catalyst. One was synthesized by a sol−gel condensation reaction without the addition of a solvent, as described in a previous paper (GD50) (11). Another was prepared with sol−gel condensation in the presence of a solvent, *N*,*N*-dimethylacetamide (DMAc; 99%, Aldrich) as a reaction medium (HGD50). For the synthesis of HGD50 oligosiloxane, DPSD was dissolved in DMAc to obtain a clear solution over 30 min at room temperature, and then GPTS and $Ba(OH)_2 \cdot H_2O$ were added in this solution. The final solution was reacted at 70 °C over 2 weeks under reflux conditions. These reaction schemes are shown in Scheme 1. In the case of GD50 oligosiloxane, DPSD was directly dissolved in GPTS with $Ba(OH)_2 \cdot H_2O$. Subsequently, methanol, which was the byproduct of the sol−gel condensation reaction of the organosilanes, was removed by vacuum heating. Both reactant compositions had a 1:1 molar ratio of GPTS and DPSD, and the formulation is listed in Table 1. The solution was then cooled to room temperature and filtered through a 0.45-μm-diameter Teflon filter to remove $Ba(OH)_2 \cdot H_2O$.

Characterization of Highly Condensed Epoxy−Oligosiloxane Resins. The formation of siloxanes and preservation of the epoxy rings in the synthesized epoxy−oligosiloxane resins were characterized using ^{29}Si and ^{1}H NMR spectroscopy (Bruker FT 500 MHz), respectively, with a sample consisting of 30 vol % of the resin in chloroform-*d*. Chromium(III) acetylacetonate as a relaxation agent of silicon was added at a concentration of 30 mg L^{-1}. Fourier transform infrared (FT-IR) spectroscopy (Jasco FT-IR 680plus) was also measured with a resolution of 4 cm^{-1} in the wavenumber range 400−4000 cm^{-1}. The distribution of molecular species in the epoxy−oligosiloxane resins was examined by matrix-assisted laser desorption and ionization time-of-flight mass spectrometry (MALDI-TOF MS). The spectra of MALDI-TOF MS were obtained with a Voyager-DE STR 4700 proteomics analyzer (PerSeptive Biosystems) equipped with a nitrogen laser using a wavelength of 337 nm and a pulse width of 3 ns. To prepare the samples for MALDI-TOF MS, 2,5-dihydroxybenzoic acid (Aldrich) and acetone were used as the matrix and solvent, respectively. In addition, the molecular size of the synthesized epoxy−oligosiloxanes was measured by using small-angle X-ray scattering (SAXS). SAXS patterns were measured using a 1.608 Å synchrotron X-ray source (2.5 GeV, beamline 4C1, Pohang Accelerator Laboratory, Republic of Korea). The scattering vector ranged between 0.01 and 0.2 $Å^{-1}$. The nanosize of the epoxy−oligosiloxanes with a wide distribution of molecular weights was characterized from the radius of gyration (R_g) quantized by a Guinier plot of SAXS. Epoxy−oligosiloxanes were diluted with 2-butanone (98%, Aldrich) in a 0.7 mm mica window.

Fabrication and Characterization of Epoxy−Hyrimer Coating Films. To fabricate epoxy−hybrimer coating films based on GD50 and HGD50 oligosiloxane resins, we used methyl tetrahydrophthalic anhydride (MeTHPA; Kukdo Chem.) as a thermal curing agent and *N,N*-dimethylbenzylamine (BDMA; 99%, Aldrich) as a catalyst to promote thermal curing. The equivalent molar ratio between epoxy−oligosiloxane and anhydride was 1:1, and the amount of BDMA was at 4 mol % in anhydride. The resins were diluted in propylene glycol methyl ether acetate (PGMEA; 99%, Aldrich) to fabricate hybrimer coating films. The weight of added PGMEA was 1.5 and 2 times compared to those of GD50 and HGD50 oligosiloxane resins, respectively. The mixed solution was stirred at room temperature for 2 h. Then, the solution was spin-coated at 3000 rpm for 30 s on the ITO glass. The coating films were thermally cured at 200 °C for 24 h with a heating rate of 5 °C min^{-1}. A Au electrode of sphere shape with a radius of 0.54 mm for electrical characterization was deposited by thermal evaporation with a deposition rate of 0.5 Å min^{-1}.

The electrical properties of the epoxy−hybrimer coating films such as the leakage current density and dielectric constant were examined with an HP4194A (Agilent Technologies) impedance/gain analyzer and a Keithley 237 source-measure unit (Keithley).

The transmission spectrum of the hybrimer coating film prepared by HGD50 on a quartz substrate was obtained in a wavelength between 300 and 800 nm using an ultraviolet−visible−near-infrared (UV/vis/NIR) spectrophotometer (Shimadzu, UV3101PC). We used the bare quartz substrate as a reference to measure the transmission spectrum. The refractive index of the hybrimer coating film by HGD50 was measured using a prism coupler (Metricon, 2010) at a wavelength of 632.8 nm.

RESULTS AND DISCUSSION

Formation of Highly Condensed Epoxy−Oligosiloxane Resins. We measured ^{29}Si NMR spectroscopy to confirm siloxane formation and calculate the DOC of GD50 and HGD50 oligosiloxanes (Figure 1a). D^n and T^n represent the notations of Si from DPSD and GPTS, respectively. The superscript "n" means the number of siloxane bonds of the Si atoms. In Figure 1, D^0 (−29 ppm) and T^1 (−49 to −51 ppm) of HGD50 are completely removed, D^1 (−36 to −38 ppm) and T^2 (−57 to −61 ppm) decrease relative to those of GD50, and D^2 (−42 to −47 ppm) and T^3 (−65 to −69 ppm) of HGD50 dramatically increase. The increment of D^2 and T^3 with many siloxane bonds means that a high DOC is obtained for the formation of oligosiloxanes (12−14).

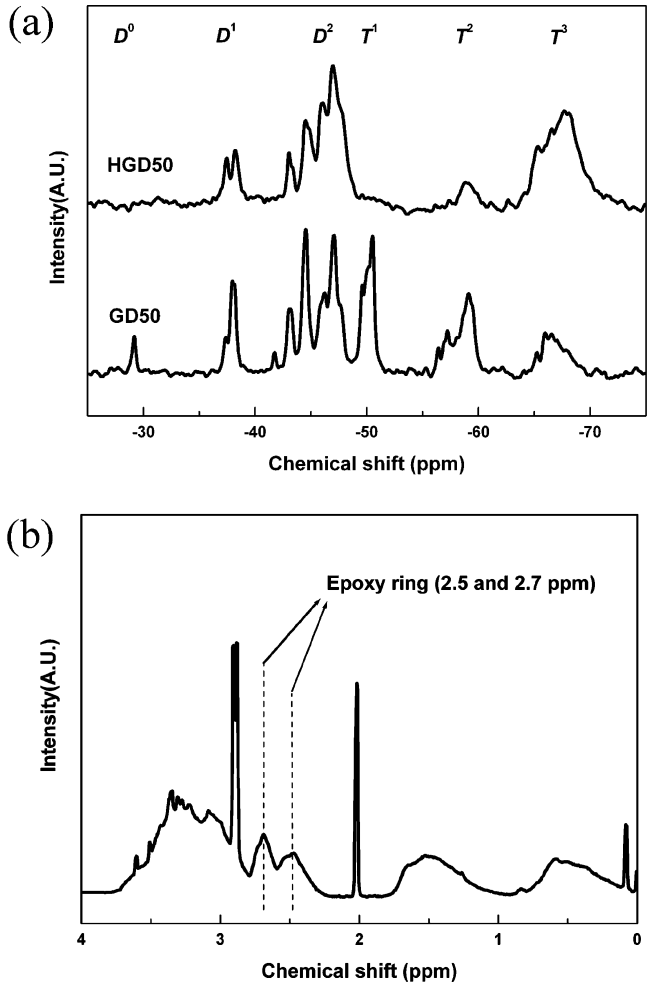

FIGURE 1. (a) ^{29}Si NMR spectra of epoxy−oligosiloxane resins. (b) ^{1}H NMR spectrum of a highly condensed epoxy−oligosiloxane resin.

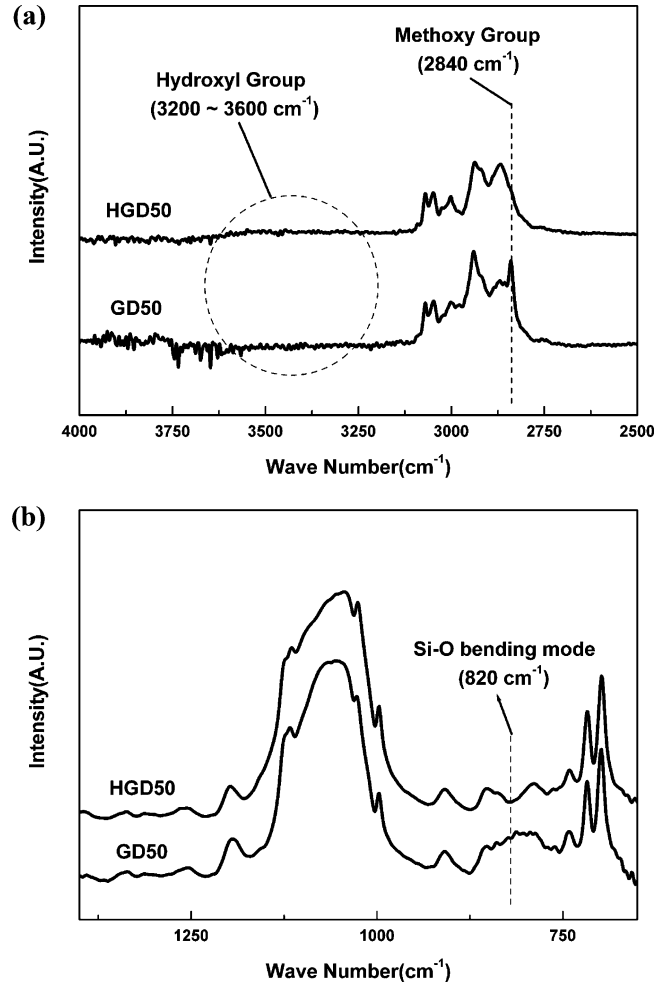

FIGURE 2. FT-IR spectra of epoxy−oligosiloxane resins.

Consequently, the DOCs of GD50 and HGD50 oligosiloxanes can be calculated using the following equation (15).

$$\mathrm{DOC} = \frac{D^1 + 2D^2 + T^1 + 2T^2 + 3T^3}{2(D^0 + D^1 + D^2) + 3(T^0 + T^1 + T^2 + T^3)} \times 100$$

The DOCs of GD50 and HGD50 oligosilaxanes are 73% and 93%, respectively. As expected, the DOC of HGD50 increases 20% compared to that of GD50. The oligosiloxane resins can be synthesized by a condensation reaction between silanol groups of DPSD and methoxy groups of GPTS. Because the condensation reaction is limited by the viscosity of synthesized oligosiloxane resins, the high viscosity of the GD50 oligosiloxane resin, which was synthesized without the addition of a solvent, results in a low DOC. On the other hand, the presence of a solvent in the condensation reaction causes the resin to be fluid, promoting the reaction to produce highly condensed oligosiloxane. This causes the solvent to act as a reaction medium and enhances the reaction to make the increment of the DOC.

The ^{1}H NMR spectrum of a HGD50 oligosiloxane resin was measured to confirm the preservation of the epoxy ring. Figure 1b represents the ^{1}H NMR spectrum of the synthesized HGD50 oligosiloxane resin. The chemical shifts of the epoxy ring in the HGD50 oligosiloxane resin show at 2.5 and 2.7 ppm. The chemical shift of H atoms at the C atom directly bonded to the Si atom shows at 0.5 ppm. When the area of the peak at 0.5 ppm is compared with the sum area of the peaks at 2.5 and 2.7 ppm, it is possible to verify preservation of the epoxy ring because two bands have the same number of H atoms. The difference between the peak areas at 0.5 ppm and the sum area of the peaks at 2.5 and 2.7 ppm does not exist in the ^{1}H NMR spectrum of the HGD oligosiloxane resin. Depending on this result, we confirm that the epoxy ring of the HGD oligosiloxane resin was preserved without cleavage (11).

Figure 2 shows the FT-IR spectra to support the results of the ^{29}Si NMR spectra. In the FT-IR spectra, the hydroxyl group (3200−3600 cm^{-1}) is completely removed and the Si−O−Si asymmetric stretching mode is shown at 1110 and 1065 cm^{-1} in both of the GD50 and HGD50 oligosiloxane resins (16, 17). On the other hand, the methoxy group peak at 2840 cm^{-1} and the Si−O bending mode band at 820 cm^{-1} in HGD50 are smaller than those in GD50 (4, 18). This represents the theory that unreacted methoxy groups are converted into siloxane bonds because of promotion of the condensation reaction. Thus, it is confirmed that the condensation reaction is promoted and more siloxane bonds

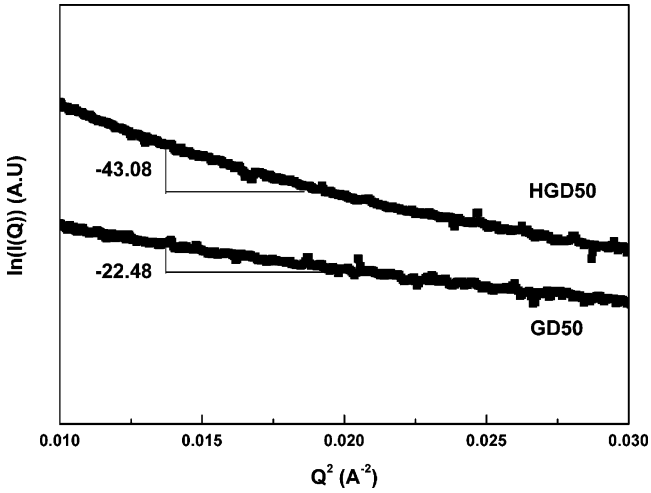

FIGURE 3. SAXS Guinier plots (ln[$I(Q)$] vs Q^2) of epoxy−oligosiloxanes.

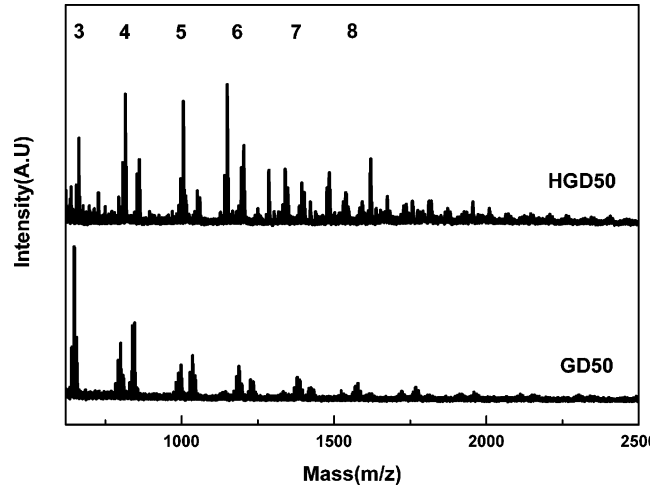

FIGURE 4. MALDI-TOF MS spectra of epoxy−oligosiloxane resins. Peaks corresponding to trimer, tetramer, pentamer, hexamer, heptamer, and octamer are represented, respectively.

Table 2. Radius of Gyration (R_g), Diameter of Sphere Shape ($2R_s$), and Length of Rodlike Shape (R_T) Calculated from SAXS Data

sample	R_g (nm)	$2R_s$ (nm)	R_T (nm)
GD50	0.82	2.12	2.85
HGD50	1.14	2.94	3.94

in HGD50 are formed than in GD50 because of the addition of a solvent as a reaction medium.

Molecular Size and Distribution of Epoxy−Oligosiloxanes. The sizes of the epoxy−oligosiloxanes were calculated with the radius of gyration (R_g) obtained by SAXS. R_g of the oligosiloxanes was determined by the following equation from the Guinier plots [scattered intensity $I(Q)$ vs Q^2] in the Guinier region ($0.1 < R_gQ < 1$) of the SAXS spectra (19).

$$\ln[I(Q)] = A - \frac{1}{3}Q^2R_g^2$$

The Guinier plots from the SAXS results of GD50 and HGD50 oligosiloxane resins are shown in Figure 3. The gradient of the Guinier plots of the HGD50 oligosiloxane resin negatively increases, meaning that R_g of HGD50 oligosiloxanes is higher. The real molecular size was calculated by R_g from the Guinier plots with the following equations depending on their shapes.

$$\text{sphere shape } R_g = \sqrt{\frac{3}{5}}R_s$$

$$\text{rodlike shape } R_g = \sqrt{\frac{1}{12}}R_T$$

R_s is the radius of the spherical resin, R_T is the length of the thin rodlike resin, and R_g is the radius of gyration. The calculated $2R_s$, R_T, and R_g are listed in Table 2. As summarized in Table 2, it is confirmed that the molecular size of HGD50 oligosiloxanes is larger than that of GD50. This is because the formation of more siloxane bonds by using a solvent as a reaction medium causes the increased size of the HGD50 oligosiloxanes.

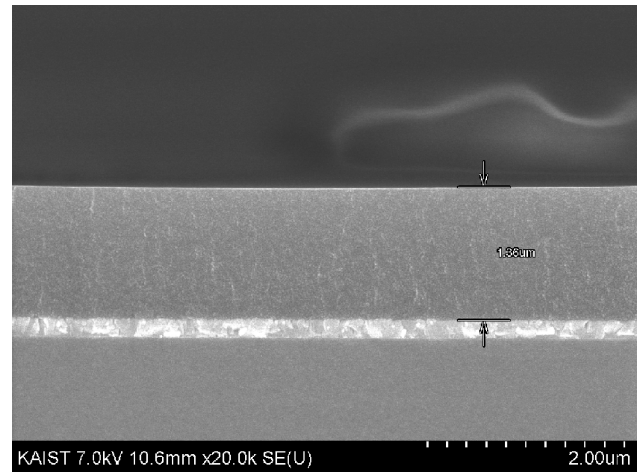

FIGURE 5. Cross-sectional SEM image of epoxy−hybrimer coating films.

We measured MALDI-TOF MS to support the SAXS results and confirm that HGD50 oligosiloxanes have species with high molecular weights. Figure 4 represents the results of MALDI-TOF MS of GD50 and HGD50 oligosiloxane resins. The MALDI-TOF MS peaks of HGD50 oligosiloxane resins are shifted to peaks of species with high molecular weights compared to those of GD50 oligosiloxane resins.

Electrical Properties of Epoxy−Hybrimer Coating Films. GD50 and HGD50 oligosiloxane resins, which were diluted in PGMEA, were spin-coated on the ITO glass substrates and thermally cured to fabricate hybrimer coating films. The film thickness can be controlled depending on the concentration of the oligosiloxane resin in PGMEA and was finally fixed at around 1.5 μm for electrical characterization. As shown in Figure 5, the epoxy−hybrimer coating films are dense, uniform, and crack-free with good adhesion with the ITO electrode.

We examined electrical properties such as the leakage current density and dielectric constant of the epoxy−

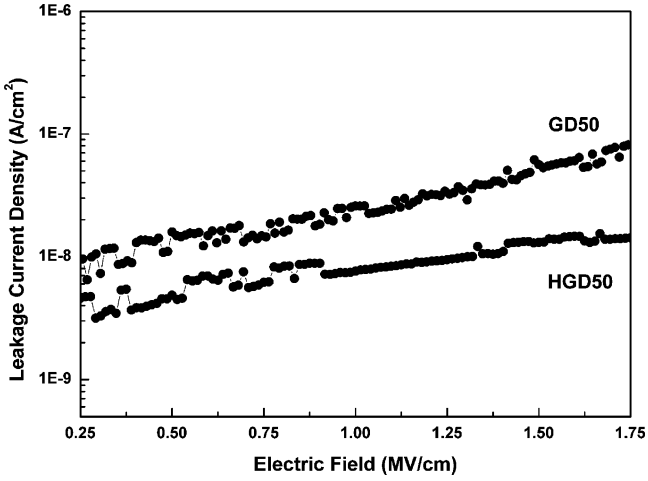

FIGURE 6. Leakage current density of epoxy−hybrimer coating films.

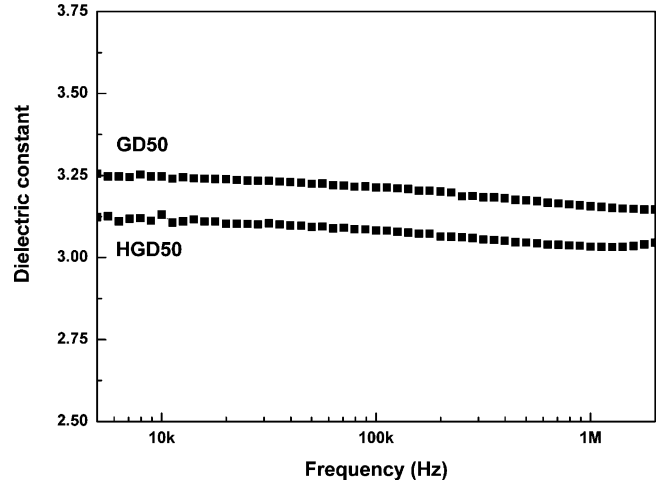

FIGURE 7. Dielectric constant variation of hybrimer coating films as a function of the frequency.

hybrimer coating films. Figure 6 shows the dependence of the leakage current density of the GD50 and HGD50 hybrimer coating films depending on the applied electric field. The leakage current densities at 1 MV cm^{-1} of the GD50 and HGD50 hybrimer coating films were 25.9 and 7.6 nA cm^{-2}, respectively. The leakage current density of the epoxy−hybrimer coating films is lower than those of soluble polymers such as poly(4-vinylphenol), which were reported to have a relatively high leakage current density of around 10^{-7} A cm^{-2} at 1 MV cm^{-1} (20). Also, the leakage current density of the HGD50 hybrimer coating film was lower than that of the previously reported siloxane-based low-*k* dielectric materials (3). The leakage current density of HGD50 hybrimer coating films improved relative to that of GD50 hybrimer coating films. Because more condensed oligosiloxanes cause larger-sized oligosiloxanes, the HGD50 hybrimer coating film shows enhanced insulating properties compared to the GD50 hybrimer coating film.

Because the performance of TFT is improved by the reduction of the capacitive coupling in the dielectric layer, it is advisible to have a low dielectric constant of dielectric coating films. Figure 7 represents the variation of the dielectric constant of the GD50 and HGD50 hybrimer coating films as a function of the frequency. The dielectric constants of GD50 and HGD50 hybrimer coating films at 1 MHz are 3.16 and 3.03, respectively, which are lower than that of SiO_2 film (3.9). The lower dielectric constant of HGD50 hybrimer coating films than that of GD50 hybrimer coating films can be explained by the following Clausius−Mossotti relationship (21).

$$\frac{\varepsilon_r - 1}{\varepsilon_r + 2} = \frac{\rho}{M}\frac{N_0}{3\varepsilon_0}\alpha$$

ε_r is the dielectric constant, ρ is the density, N_0 is Avogadro's number, M is the molecular weight, ε_0 is the vacuum permittivity, and α is the polarizability.

From the Clausius−Mossotti relationship, the dielectric constant of materials decreases with a decrease in the density of the materials because a decrease of the density means a reduction of the number of ions or dipoles contributing to the polarizability of the materials. Because the molecular size of HGD50 oligosiloxanes, which was obtained from SAXS results shown in Figure 3 and Table 2, is larger than that of GD50 oligosiloxanes, a larger free volume of the HGD50 hybrimer coating film reduces the dielectric constant according to the Clausius−Mossotti relationship (22, 23). Also, HGD50 oligosiloxanes are more symmetric than GD50 oligosiloxanes because dipoles originating by asymmetry between methoxy group and siloxane bonds are diminished with the increased D^2 and T^3 of HGD50 in the ^{29}Si NMR spectra and the decreased methoxy peak (2840 cm^{-1}) and Si−O bending mode (810 cm^{-1}) of HGD50 in the FT-IR spectra. The increment of symmetric oligosiloxanes is induced to decrease the dielectric constant of the HGD50 hybrimer coating film.

Optical Transparency of the Epoxy−Hybrimer Coating Film. For application to the passivation layer in AMLCDs with high resolution and brightness, the passivation layer should be transparent. The transmittance spectrum of the HGD50 hybrimer coating films with improved electrical properties compared to GD50 is shown in Figure 8. The HGD50 hybrimer coating film exhibits excellent transmittance over 90% in the visible range and is colorless, as was already reported in previous studies (10, 11). The refractive index of the HGD50 hybrimer coating film is 1.56, which is comparable with that of glass, so it is suitable to reduce the efficiency loss by internal reflection.

CONCLUSION

The highly condensed epoxy−oligosiloxane resin was successfully synthesized by a sol−gel condensation reaction from GPTS and DPSD in the presence of a solvent as a reaction medium. The highly condensed epoxy−oligosiloxane had a larger molecular size and more species with high molecular weight compared to epoxy−oligosiloxanes with low DOC. It was possible to fabricate an epoxy−hybrimer coating film with a thickness of around 1.5 μm by spin coating and thermal curing. Electrical properties such as the

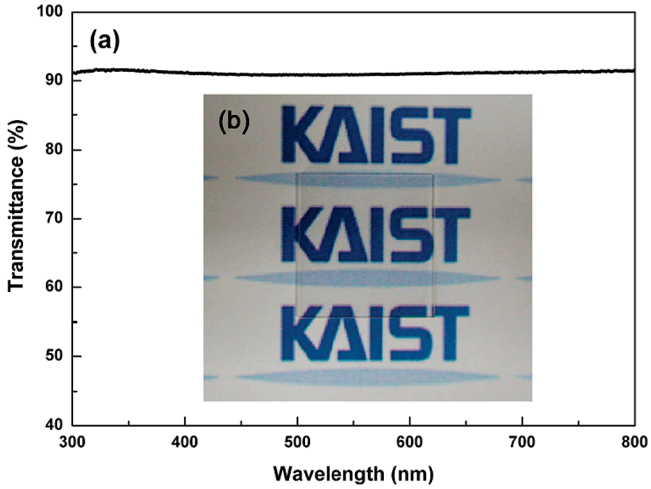

FIGURE 8. (a) Transmittance spectrum of HGD50 hybrimer coating films. (b) Photograph of the HGD50 hybrimer coating film.

leakage current density and dielectric constant of the hybrimer coating film fabricated by a highly condensed epoxy−oligosiloxane resin were superior to those of the hybrimer coating film by an oligosiloxane resin with low DOC. We also verified that the fabricated hybrimer coating film had a high transmittance of over 90%. Therefore, the hybrimer coating film of a highly condensed epoxy−oligosiloxane resin can be employed as the passivation layer in the TFT.

Acknowledgment. This work was supported by a Korea Science and Engineering Foundation (KOSEF) grant funded by the Korean government (MEST) (Grants R11-2007-045-03002-0 and R01-2007-000-20815-0). We thank the Pohang Accelerator Laboratory in the Republic of Korea for use of its beamline 4C1.

REFERENCES AND NOTES

(1) Katayama, M. *Thin Solid Films* **1999**, *341*, 140–147.
(2) Matsumura, H. *J. Appl. Phys.* **1989**, *66*, 3612–3617.
(3) Krishnamoorthy, A.; Spear, R.; Gebrebrhan, A.; Stifanos, M.; Bien, H.; Lowe, M.; Yellowaga, D.; Smith, P.; O'Rourke, S.; Loy, D.; Dailey, J.; Marrs, M.; Ageno, S. *SID2008 DEGEST* **2008**, 140–142.
(4) Sivoththaman, S.; Jeyakumar, R.; Ren, L.; Nathan, A. *J. Vac. Sci. Technol. A* **2002**, *20*, 1149–1153.
(5) Chang, T.-S.; Chang, T.-C.; Liu, P.-T.; Chang, T.-S.; Tu, C.-H.; Yeh, F.-S. *IEEE Electron Devices L* **2006**, *27*, 902–904.
(6) Chang, T.-S.; Chang, T.-C.; Liu, P.-T.; Tsao, S.-W.; Yeh, F.-S. *Thin Solid Films* **2007**, *516*, 374–377.
(7) Eo, Y. J.; Kim, J. H.; Ko, J. J.; Bae, B. S. *J. Mater. Res.* **2005**, *20*, 401–408.
(8) Kim, J. K.; Kang, D. J.; Bae, B. S. *Adv. Funct. Mater.* **2005**, *15*, 1870–1876.
(9) Kang, D. J.; Kim, W. S.; Bae, B. S. *Appl. Phys. Lett.* **2005**, *87*, 221106.
(10) Lee, T. H.; Kim, J. H.; Bae, B. S. *J. Mater. Chem.* **2006**, *16*, 1657–1664.
(11) Yang, S. C.; Kim, J. H.; Jin, J. H.; Bae, B. S. *J. Polym. Sci., Polym. Phys.* **2009**, *47*, 756–763.
(12) Jermouni, T.; Smaihi, M.; Hovnanian, N. *J. Mater. Chem.* **1995**, *5*, 1203–1208.
(13) Brunet, F. *J. Non-Cryst Solids* **1998**, *231*, 58–77.
(14) Hoebbel, D.; Reinert, T.; Schmidt, H. *J. Sol−Gel. Sci. Technol.* **1996**, *7*, 217–224.
(15) Sepeur, S.; Kunze, N.; Werner, B.; Schmidt, H. *Thin Solid Films* **1999**, *351*, 216–219.
(16) Innocenzi, P.; Brusatin, G.; Guglielmi, M.; Bertani, R. *Chem. Mater.* **1999**, *11*, 1672–1679.
(17) Ou, D. L.; Seddon, A. B. *J. Non-Cryst. Solids* **1997**, *210*, 187−203.
(18) Shirosakia, Y.; Tsurua, K.; Hayakawaa, S.; Osakaa, A.; Lopes, M. A.; Santos, J. D.; Fernandes, M. H. *Biomaterials* **2005**, *26*, 485–493.
(19) Roe, R. J. *Methods of X-ray and Neutron Scattering in Polymer Science*; Oxford University Press: New York, 2000; p 155.
(20) Klauk, H.; Halik, M.; Zschieschang, U.; Schmid, G.; Radlik, W.; Weber, W. *J. Appl. Phys.* **2002**, *92*, 5259–5263.
(21) Smyth, C. P. *Dielectric Behavior and Structure*; McGraw-Hill Book Co.: New York, 1955; p 5.
(22) Simpson, J. O.; St. Clair, A. K. *Thin Solid Films* **1997**, *308−309*, 480–485.
(23) Kim, H. J.; Shao, Q.; Kim, Y.-H. *Surf. Coat. Technol.* **2003**, *171*, 39–45.

AM900252V